COAGULANT PREPARATION FROM GLUTARALDEHYDE-CROSSLINKED DURIAN SKIN CELLULOSE FOR TREATMENT OF WASTEWATER GENERATED BY SUGAR PALM STARCH INDUSTRIES

SIGIT PRIATMOKO,[*] DANTE ALIGHIRI,[*] APRILIANA DRASTISIANTI,[**] DEWANTO HARJUNOWIBOWO,[***] ALFIAN NUR ROHMAN[*] and TRIASTUTI SULISTYANINGSIH[*]

[*]*Chemistry Department, Faculty of Mathematics and Natural Sciences, Universitas Negeri Semarang, Indonesia*
[**]*Department of Chemistry Education, Faculty of Sciences and Technology, Universitas Islam Negeri Walisongo Semarang, Indonesia*
[***]*Department of Physics Education, Faculty of Teacher Training and Education, Universitas Sebelas Maret, Indonesia*
✉ *Corresponding author: D. Alighiri, dante_alighiri@mail.unnes.ac.id*

Received May 15, 2023

Arenga pinnata starch (APS) production from APS industrial centers in Klaten, Indonesia, produces *Arenga pinnata* starch mill effluent (APSME). This waste will undoubtedly harm the environment, significantly reducing river water quality. On the other hand, in Gunungpati, Semarang, Indonesia, durian fruit is abundant, it leaves durian skin waste, which may cause environmental pollution. However, durian skin contains cellulose, which has the potential to be valorized for various applications. Therefore, this study evaluated the preparation of natural coagulant from durian skin cellulose crosslinked with glutaraldehyde for treating APSME from APS industrial centers in Klaten, Indonesia. Durian skin flour (DSF), durian skin cellulose (DSC), and glutaraldehyde-crosslinked durian skin cellulose (DSC-G) coagulants were characterized by proximate composition, UV-Vis spectroscopy, Fourier-transform infrared (FTIR) spectroscopy and scanning electron microscopy (SEM). The effects of coagulant dose, pH, and mixing speed on removal efficiency and sludge volume in DSF, DSC, and DSC-G were compared with polyaluminum chloride (PAC). The study assessed the process efficiency in terms of percentage removals for chemical oxygen demand (COD), biological oxygen demand (BOD_5), total dissolved solids (TDS), and total suspended solids (TSS) as 71.38%, 78.23%, 94.79%, and 96.12%, respectively, with a percentage sludge volume of 24%. The results indicated that the optimum DSC-G dosage was 2500 mg/L with an optimum working area of pH at 5.5 and a mixing speed of 90 rpm. DSC-G has a floc stability of -12.33 mV. This study indicated that DSC-G has the potential to be used as a coagulant for the treatment of APSME.

Keywords: coagulant, *Arenga pinnata*, cellulose, durian skin, glutaraldehyde

INTRODUCTION

Palm fiber is a natural fiber derived from sugar palm trees (*Arenga pinnata* Merr.), which are annual plants indigenous to tropical Asia.[1] They can attain a height of 15–20 m and a stem diameter of up to 65 cm, with a leaf canopy that rises above the stem.[2] The surface of the stem is covered with palm fibers that originate at the stem's base. Additionally, nearly all sugar palm plant parts are beneficial. It is a source of food, industrial materials, and renewable energy. A variety of goods can be produced from it, including fresh palm juice, brown sugar, vinegar, palm wine, bioethanol, and black fiber. In addition, its trunk is made of tough and durable wood that can be used for furniture manufacturing, brooms, handicrafts, housing construction, waterproof transportation, and rope materials, among other things.[3,4] According to Ishak *et al*.,[5] the root of *Arenga pinnata* has medicinal value. India, Malaysia, Indonesia, the

Philippines, and China all contribute to its production area. This plant is renowned for its many economic applications.[4] It also has a high hydrological function, which makes it an ideal plant for conservation. In Indonesia, sugar palm tree trunks are used as a raw material to produce *Arenga pinnata* starch (APS), preferably after the tree has ceased producing sugar and fruit. [6,7] 10–20 trees are required to produce one tonne of starch, indicating that, on average, each tree can produce 50–100 kg of starch. APS contains a high proportion of amylose.[5] One of the APS production centers in Indonesia is located in Klaten Regency, Central Java Province. The APS industries are increasing rapidly and are the mainstay of the local population.

In the APS production process, this industry produces liquid and solid waste. Such waste will undoubtedly harm the surrounding environment, significantly reducing river water quality. Therefore, to dispose of the waste, it must be processed first to be safe for the environment. According to Firdayati and Handayani,[8] palm flour liquid waste still contains starch and fiber, both dissolved and suspended. The value of BOD (biological oxygen demand) is 2222 mg/L, and COD (chemical oxygen demand) is 5721.5 mg/L. However, unfortunately, all APS industrial centers in Klaten, Central Java, Indonesia, are micro and small enterprises that cannot process waste. Expensive waste treatment costs are an obstacle the industry cannot overcome. Therefore, it is necessary to find a way to create new materials for waste treatment that are cheap and effective. This waste will be referred to as *Arenga pinnata* starch mill effluent (APSME) in this study.

Wastewater treatment can be done by various methods, such as precipitation, adsorption, and coagulation. Among the existing methods, the coagulation method is one of the most widely applied and a relatively inexpensive method among wastewater treatment systems.[9,10] A synthetic coagulant is usually used in this method. Commonly used coagulants are aluminum salts, such as aluminum sulfate and poly aluminum chloride (PAC). However, using synthetic coagulants produces adverse environmental effects, and the price is still relatively high if applied on a large scale in wastewater treatment, especially in small industries. Other studies have also revealed that synthetic coagulants can cause various health problems, if not appropriately managed, because of the toxic effects of metals on human health, causing allergies, tumors, and cancer. Therefore, there has been a rising interest in the use of natural coagulants to reduce the amounts of synthetic ones.[11]

One of the potential natural materials that can be used in this case is cellulose, which is abundantly available in nature, especially from agricultural waste.[12-14] In Indonesia, there are huge amounts of farming waste, which contains high amounts of cellulose, but it hasn't been valorized so far. Durian skin waste is one of such residues that cause problems for the environment. Durian fruit (*Durio zibethinus* Murr.) is one of the most popular and widely consumed fruits in Southeast Asia, particularly Malaysia, Indonesia, Thailand, and the Philippines. This durian fruit is abundant and widespread in Central Java, Indonesia. The durian fruit consists of pulp, seeds and skin. Only 15-30% of the total weight of the fruit is edible, and the remaining 70-85%, in the form of skin and seeds, represent waste that may cause environmental problems, when dumped in landfills.

Every durian season, there is undoubtedly a lot of durian waste, especially from durian skin. However, durian peel contains 60.5% cellulose, 13.1% hemicelluloses and 15.45% lignin.[13-15] Because it has a lot of cellulose, it is a good source for the development of many value-added products that can be used in many ways.[16,17] Cellulose is a natural polymer, with numerous excellent characteristics, such as low density, lightweight, and adjustable surface chemistry, which is of particular importance in wastewater treatment.[18] To reduce the adverse impacts of APSME, this study aims to evaluate natural coagulation based on durian cellulose crosslinked with glutaraldehyde through coagulation-flocculation. Before biological treatment, coagulation-flocculation is a pre-treatment method that can significantly reduce the effluent's total pollution strength.[19]

EXPERIMENTAL

Material

The durian (*Durio zibethinus* Murr.) skin waste was obtained from Gunungpati, Semarang City, Central Java Province, Indonesia. The waste of *Arenga pinnata* starch (APS) was obtained from APS industrial centers in Klaten District, Central Java, Indonesia. Poly aluminum chloride, PAC (CAS number: 1327-41-9) was obtained from Bratachem, Semarang, Indonesia. Glutaraldehyde was purchased from Merck (Germany)

and used as a cross-linking agent. The reagents and chemicals used in this study, such as acetone, glutaraldehyde, ethanol, *n*-hexane, H_2SO_4 (sulfuric acid), HCl (hydrochloric acid), NaOH (sodium hydroxide), H_2O_2 (hydrogen peroxide), NaCl (sodium chloride), $CuSO_4$ (copper sulfate), Na_2SO_4 (sodium sulfate), methyl red indicator, and methyl blue indicator, were all purchased from Merck (Germany). These substances were pure analytical reagents that were not further purified.

Durian skin flour preparation

The durian skin scraps were washed with water and dried at 50 to 60 degrees Celsius (°C) for 60 minutes. The dried durian skin waste was pulverized using a grinder machine. The durian skin flour (DSF) was then sieved with a sieve size of 100 mesh. DSF that passed the 100 mesh sieve was dried at 60 °C, weighed to a constant weight, and used as a sample for further treatment.[13,14]

Cellulose isolation

DSF was separated from the starch by soaking in hot water (80-100 °C) for 15 minutes. Resins, waxes, and other extracts were extracted by refluxing toluene and ethanol (2:1) for five hours, then filtered and the retained material was dried. 5 grams of extract-free biomass was weighed into a 250 mL beaker and leached with 200 mL of 0.1 M HCl at 100 °C for 2 hours while stirring. The mixture was subsequently filtered, and the cellulose-lignin-rich insoluble residue was washed with 20 mL of deionized water and air-dried overnight. The cellulose-lignin-rich residue was delignified by soaking it in a 10% (w/v) sodium hydroxide solution for 24 hours. The mixture was then filtered, and the cellulose-rich residue was washed until the solution was neutral with 20 mL of 0.1 M HCl and distilled water. The obtained crude cellulose was filtered and dried. Before bleaching, the crude cellulose was air-dried overnight.[12-14,20] The amount of cellulose in the initial sample was equivalent to the weight of the bleached cellulose as a percentage of the DSF sample's weight. This is referred to as durian skin cellulose (DSC) in this study.

Preparation of DSC crosslinked with glutaraldehyde (DSC-G)

10 g of DSC was reacted with 600 mL NaOH 0.07 M for 1 h under agitation, and the solution was crosslinked with glutaraldehyde in different DSC/glutaraldehyde ratios of 1:1-1:5 w/w. The crosslinking reaction was carried out for 30 min. The mixture was cooled to 30 °C for 4 h under agitation, and 5 g of NaCl was added. The pH of the mixture was adjusted to 7 using distilled water and mixed for 1 h. The solid that formed was filtered with Whatman paper on a Buchner funnel and dried in an oven at 55 °C until constant weight.[21-23]

Characterization sample

The samples were characterized in terms of proximate composition, and by UV-Vis spectroscopy, FTIR (Fourier transform infrared) spectroscopy, and SEM (scanning electron microscopy). FTIR analyses were conducted on a Perkin Elmer Spectrum Version 10.03.06 FT-IR spectrophotometer. In a mortar, 1 g of powder samples were crushed with 10 g of KBr (sample: KBr in a ratio of 1:10), mixed evenly, and then pressed into pellets. The next step is to press the mold until a transparent pellet is produced. The pellets were then analyzed with a Perkin Elmer Spectrum FT-IR spectrophotometer, version 10.03.06. The spectrum is described as a transmittance curve at wavenumbers 4000-200 cm^{-1}.[24] A Phenom ProX SEM (Thermo Scientific) was to examine the surface morphology of the samples. The samples were coated with carbon and gold, before recording the SEM images.

Wastewater sampling

The wastewater used for this study was APSME, obtained from APS industrial centers in Klaten District, Central Java, Indonesia. The APSME sample was sealed and stored in a labelled, thermally-resistant plastic container. To avoid biodegradation due to microbial action, samples were cooled to approximately 4 °C for storage. Before beginning the experiments, the preserved samples were allowed to reach room temperature at 27–30 °C and analyzed for their characteristics and chemical properties. The APSME was defined and employed in the jar tests.[24] The following parameters were used to characterize the wastewater: pH, TSS, TDS, BOD_5, COD and temperature.[26-32]

Jar test

During the investigation, a standard jar test device was used to coagulate fresh APSME with PAC, DSF, DSC, and DSC-G. The initial concentration of the APSME samples was determined by measuring the pH, TSS, TDS, BOD_5, COD, and temperature. The samples were homogeneously mixed and distributed into beakers containing 1000 mL of suspension each. The doses of coagulants were optimized. Each coagulant was put in a centrifuge and then rotated at a speed of 300 rpm for 2 minutes, followed by 60 rpm for 20 minutes.[33] Sampling was carried out after settling for 30 minutes, and then the pH, TSS, TDS, BOD_5, COD and temperature were measured. From these results, the optimum coagulant dose was determined.[26-32] The floc formed from the optimum coagulant was analyzed by SEM to determine its morphological characteristics, and by SEM-EDX to determine the composition of the floc.

Zeta potential

A Horiba SZ-100 (Horiba, Ltd., Japan) was used to measure the zeta potential of the samples

(measurement conditions: holder temperature: 24.9 °C, dispersion medium viscosity: 0.897 mPa.s, conductivity: 223.593 mS/cm, and electrode voltage: 0.8 V). The samples for zeta potential measurement consisted of a 0.25-weight percent sample suspension with 10 mM NaCl. The addition of NaCl is required for accurate zeta potential measurements.[34] At room temperature, all zeta potential values are reported as the mean of 10 measurements involving 15 cycles each.

Statistical analysis

ANOVA (analysis of variance) was used to analyze the experimental data. Three observations were expressed as the mean standard deviation. The significance level for homogeneous groups and the least significant difference (LSD) was $p \leq 0.05$. All statistical analyses were conducted with the SPSS 24 program.

RESULTS AND DISCUSSION

Characterization of DSF, DSC, and DSC-G

In this study, the durian skin waste used as a raw material for coagulant preparation had a moisture content of about 9.37% ± 0.74 (w/w), as shown in Table 1. The most significant components of the durian skin come from carbohydrates and fiber at 21.79 ±0.20% and 53.55 ±0.53% (w/w), respectively.

This approximate value is intended for standardizing the durian skin used in this study as a coagulant material. Except for the moisture content and fiber components, which had significant differences ($p \leq 0.050$) as $p = 0.000$, the results of the analysis of the three durian skin samples were not significantly different. This difference may be because the samples taken are waste disposed of in the environment, so the state of the surrounding environment had a strong influence on them. Fiber is mainly composed of cellulose.[12-14] The Fourier Transform Infrared (FTIR) spectroscopy confirmed the presence of cellulose (Fig. 1).

Table 1
Proximate composition of durian (*Durio zibethinus*) skin waste

Component	Durian skin waste in this study (%)*			
	X	Y	Z	Mean
Crude protein[a]	5.67 ± 0.12	5.87 ± 0.21	5.80 ± 0.20	5.78 ± 0.18
Carbohydrates[b]	21.73 ± 0.18	22.00 ± 0.10	21.65 ± 0.15	21.79 ± 0.20
Crude fat[c]	0.99 ± 0.08	1.02 ± 0.07	1.07 ± 0.07	1.03 ± 0.08
Moisture content[d]	10.25 ± 0.05	8.60 ± 0.26	9.27 ± 0.25	9.37 ± 0.74
Ash[e]	8.47 ± 0.60	8.50 ± 0.10	8.48 ± 0.11	8.48 ± 0.08
Fibre[f]	52.89 ± 0.06	54.03 ± 0.10	53.73 ± 0.26	53.55 ± 0.53

*Treatment means provided by ANOVA, values were expressed as mean ± standard deviation of three replications, the mean difference is significant at $p \leq 0.050$; [a] Mean of crude protein is not significantly different for different samples at $p = 0.43$; [b] Mean of carbohydrates is not significantly different for different samples, at $p = 0.058$; [c] Mean of crude fat is not significantly different for different samples, at $p = 0.525$; [d] Mean of moisture content is significantly different for different samples, at $p = 0.000$; [e] Mean of ash is not significantly different for different samples, at $p = 0.936$; [f] Mean of fiber is significantly different for different samples, at $p = 0.000$

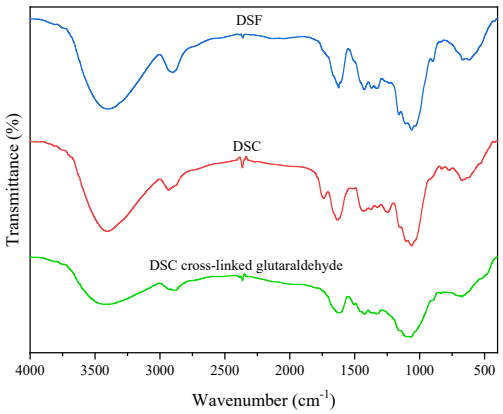

Figure 1: FTIR spectra of DSF (durian skin flour), DSC (durian skin cellulose), and DSC-G (durian skin cellulose crosslinked with glutaraldehyde)

The DSF, DSC, and DSC-G were characterized to determine the active components that act as coagulants. Coagulant characterization was carried out using the FTIR method. Based on Figure 1, the hydroxyl groups (–OH) in the DSF, DSC, and glutaraldehyde-crosslinked DSC spectra, indicating the functional groups of cellulose compounds, were noted in wavenumber range of 3200-3600 cm^{-1}. The hydroxyl groups come from the monomer that composes cellulose, namely β-1,4-glucose, which is rich in hydroxyl groups and can also arise from inter and intramolecular hydrogen bonds in the cellulose structure.[12-14,35-36] The absorption band indicating the presence of lignin and hemicellulose compounds in the sample is located at a wavelength of approximately 1750 cm^{-1}. This absorption band is visible in the DSF, DSC, and DSC-G spectra, being due to the vibration of the C=O functional group. However, this absorption band has different intensity in the three spectra. It can be seen that the absorption band at about 1750 cm^{-1} in the DSF spectrum is sharper than the one in the DSC and DSC-G spectra. The presence of lignocellulosic compounds was strongly suggested in the DSF spectrum by the sharp absorption band around 1033.85-1159.22 cm^{-1}, corresponding to the vibrational region of the C-O-C group. These aspects confirm the isolation of cellulose from durian skin. Meanwhile, the successful crosslinking of DSC with glutaraldehyde was evidenced by the difference in the absorption intensity of the hydroxyl group, which was less sharp in the DSC-G spectrum, compared to the one in the DSC spectrum, at a wavenumber around 3400 cm^{-1}.

APSME characterization

Table 2 displays the results for the initial characteristics of APSME samples. BOD_5 and COD parameters can be used to assess wastewater quality. The BOD_5/COD ratio determines the biodegradability of wastewater. For a BOD_5/COD ratio above 0.5, wastewater is biodegradable and can be efficiently treated biologically. However, if it is between 0.3 and 0.5, seeding is required to biologically treat the sample, and this method is quite time-consuming, because the microorganisms that aid in the degradation process require time to acclimate. All values obtained in Table 2 exceeded permissible limits, as can be seen. Further experimental research is conducted on the effects of various coagulants and the selected contaminants.[19,37-39]

The analysis of the three APSME samples collected from different APS industrial centers in Klaten, Central Java, did not show significantly different results, except for the pH parameter, which had significant differences ($p \leq 0.050$) at $p = 0.000$. This difference may be due to the pH of the sample, which is strongly influenced by the presence of river water and wastewater discharge.

Table 2
APSME (*Arenga pinnata* starch mill effluent) characterization

Parameter	APSME samples from industrial centers*			
	X	Y	Z	Mean
pH[a]	3.49 ± 0.015	3.39 ± 0.010	3.70 ± 0.020	3.53 ± 0.014
Temperature (°C)[b]	45.33 ± 1.53	44.00 ± 1.00	44.33 ± 2.082	44.56 ± 1.51
TDS (mg/L)[c]	45,798 ± 490.87	44,255 ± 892.19	45,310 ± 483.86	45,310 ± 483.86
TSS (mg/L)[d]	27,268 ± 305.22	28,193 ± 240.07	27,372 ± 587.37	27,611 ± 562.0
BOD_5[e]	570 ± 2.00	572 ± 2.00	568 ± 2.00	570 ± 2.45
COD[f]	1840 ± 2.00	1842 ± 2.00	1838 ± 2.00	1840 ± 2.45
BOD_5/COD	0.3097 ± 2.00	0.3105 ± 2.00	0.3090 ± 2.00	0.3097 ± 2.45

*Treatment means of ANOVA, values were expressed as mean ± standard deviation of three replications, the mean difference is significant at $p \leq 0.050$; [a] Mean of pH is significantly different for different mill effluent samples, at $p = 0.000$; [b] Mean of temperature is not significantly different for different mill effluent samples, at $p = 0.596$; [c] Mean of TDS is not significantly different for different mill effluent samples at $p = 0.066$; [d] Mean of TSS is not significantly different for different mill effluent samples at $p = 0.060$; [e] Mean of BOD_5 is not significantly different for different mill effluent samples at $p = 0.125$; [f] Mean of COD is not significantly different for different mill effluent samples at $p = 0.125$

Optimal dose of DSF, DSC, and DSC-G coagulants

Figures 2-5 show the removal efficiencies of different DSF, DSC, and DSC-G coagulants for COD, BOD_5, TDS, and TSS, and the percentage sludge volume in the APSME treatment, as well as those of PAC as a synthetic coagulant, for comparison purposes. From Figure 2, it may be noted that the optimum dose of PAC in the treatment of APSME was 3500 mg/L, with removal efficiencies for COD, BOD_5, TDS, and TSS of 65.42%, 75.11%, 96.89%, and 96.08%, respectively, and the capability for removing 16% of sludge volume.

The removal efficiency of DSF to eliminate contaminants from APSME is depicted in Figure 3 for the parameters COD, BOD_5, TDS, and TSS. It may be noted that the removal efficiency decreases as the DSF dose rises. A DSF dosage of 2500 mg/L provides the highest BOD_5 removal percentage at 40.39%, while a dosage of 3000 mg/L provides the highest COD, TDS, and TSS removal efficiencies at 45.26%, 92.22%, and 94.65%, respectively. A dosage of 3000 mg/L leads to a BOD_5 removal efficiency of 38.41%. This difference is not so significant compared to the value of 40.39% for BOD_5 removal for the dose of 2500 mg/L. Therefore, since the other parameters, such as COD, TDS, and TSS, showed the optimal removal for a dose of 3000 mg/L, it can be ignored. Thus, it can be concluded that the optimum amount of DSF to use is 3000 mg/L for the removal of 10% sludge volume.

Figure 4 depicts the effect of various DSC dosages on its removal efficiency for COD, BOD_5, TDS, and TSS, as well as the volume fraction of sludge in the APSME sample. Almost the same pattern is noticed as for DSF. However, the difference is that, for DSC, all COD, BOD_5, TDS, and TSS parameters showed the maximum values of 46.07%, 44.94%, 95.77%, and 92.29%, respectively, with 14% sludge volume removal, for the dose of 3000 mg/L.

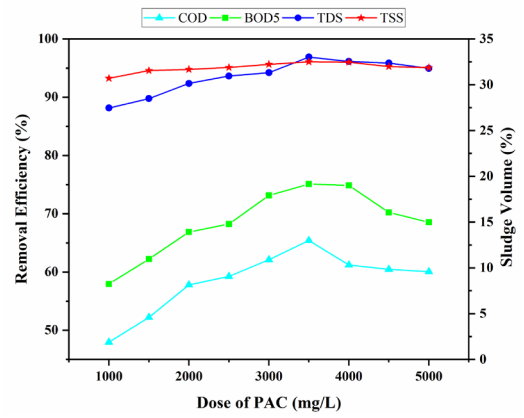

Figure 2: Removal efficiencies of PAC (poly aluminum chloride) towards APSME contaminants and sludge volume

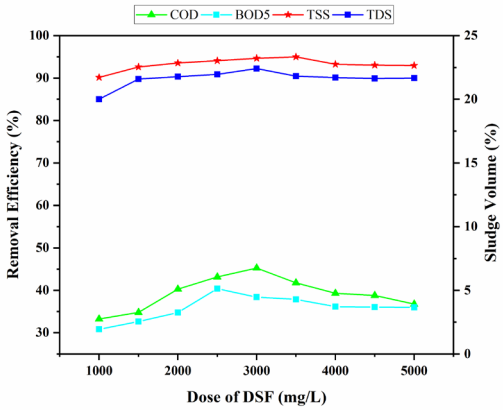

Figure 3: Removal efficiencies of DSF (durian skin flour) towards APSME contaminants and sludge volume

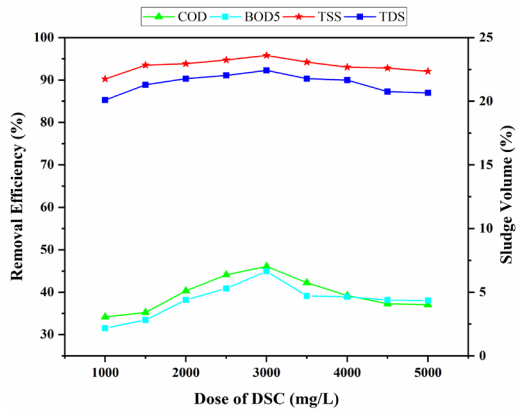

Figure 4: Removal efficiencies of DSC (durian skin cellulose) towards APSME contaminants and sludge volume

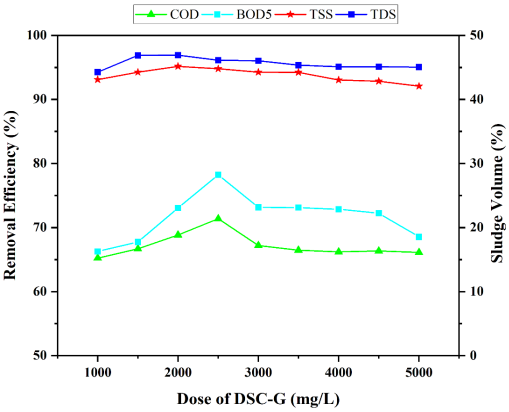

Figure 5: Removal efficiencies of DSC-G (glutaraldehyde-crosslinked durian skin cellulose) towards APSME contaminants and sludge volume

Because the main component in DSF is cellulose, as evidenced in the FTIR spectra in Figure 1, DSF and DSC show the same pattern in removing contaminants from APSME.

Figure 5 demonstrates that a DSC-G dosage of 2500 mg/L resulted in the highest removal percentages of COD, BOD_5, TDS, and TSS, and a sludge volume percentage of 24%. The pattern of removal efficiency of DSC-G shows a percentage increase, compared to DSF and DSC. Increasing removal efficiency proves that the crosslinking reaction with glutaraldehyde in the hydroxyl group of the cellulose compound, which is the main component of DSC, has been successful to produce a natural coagulant for the treatment of APSME.

Determining the optimal coagulant dosage is essential for reducing treatment process dosing costs and sludge volume.[40-42] The optimal dosages of the coagulants developed in this study were then compared to determine the smallest dose used in treating APSME, for economic considerations (Fig. 6). As may be noted in Figure 6, PAC has the highest optimal dose requirement, which is 3500 mg/L. Meanwhile, the dosage requirement for DSF and DSC was 3000 mg/L, and for DSC-G – 2500 mg/L.

TDS and TSS parameters show the same values for the four coagulants in terms of percentage removal – around 92-97%. However, the removal efficiency and sludge volume for COD and BOD_5 parameters yield different results for the coagulants. PAC and DSC-G coagulants have almost the same removal efficiency for COD and BOD_5 parameters, between 66-71% and 75-78%, respectively; but DSC-G was superior in terms of the sludge volume percentage, with 24%, while PAC showed 15%. This study suggests that DSC-G could be used as a coagulant for the treatment of APSME.

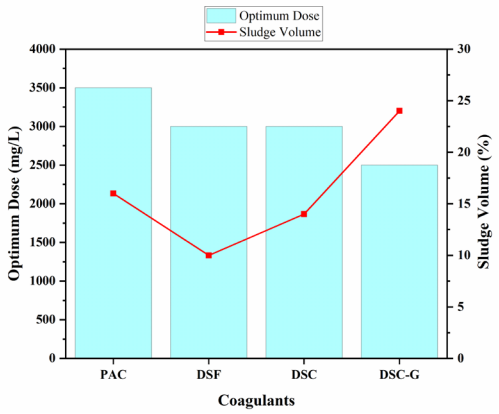

Figure 6: Comparison of optimum dose for PAC (poly aluminum chloride), DSF (durian skin flour), DSC (durian skin cellulose), and DSC-G (durian skin cellulose crosslinked with glutaraldehyde) in terms of contaminants removal efficiencies and sludge volume proportion of APSME

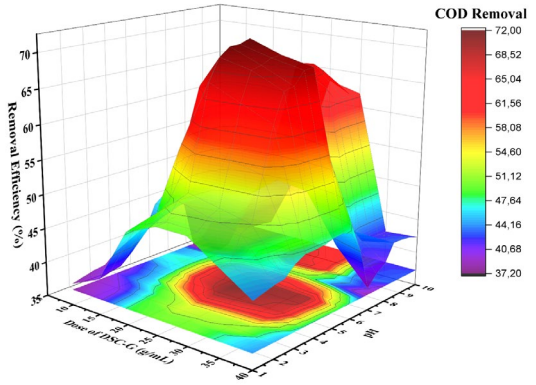

Figure 7: Interaction effects of pH and dose of DSC-G on its removal efficiency in terms of COD parameter in the treatment of APSME

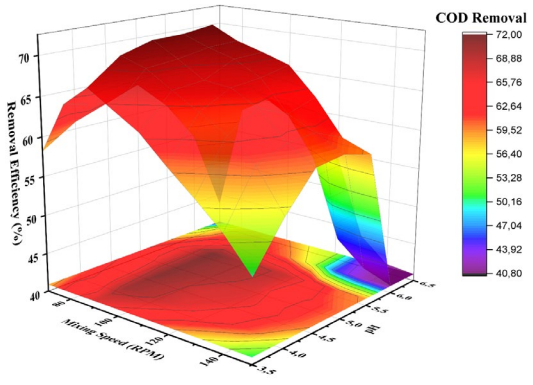

Figure 8: Interaction effects of mixing speed and pH on removal efficiency of DSC-G in terms of COD parameter in the treatment of APSME

Figure 7 illustrates the effect of DSC-G coagulant dosage and pH on COD removal by utilizing the 3D response surface plot for pH 1-10 and DSC-G coagulant dosage of 10-40 g/mL. A change in coagulant dosage in response to pH variation means a significant removal efficiency for APSME. By increasing the coagulant dosage up to 25 g/L, the percentage of COD reduction increased, but then decreased from 30 to 40 g/L, with COD removal efficiency between 72 and 65%. At a DSC-G concentration of 40 g/L, the removal efficiency decreased significantly to 47.85% for COD. In addition, these results were consistent with the contour diagram. Because of the destabilization of aggregated particles, the removal efficiency was low when the pH was below 3.5.[42,43] At pH 3, the removal efficiency began to improve, and at pH 3.5 produced significant results up to pH 5.5. At pH 6, the removal efficiency begins to decline again, and at pH 7-7.5, it falls dramatically before rising again at pH 8. At pH 7-7.5, the particle surface charge is diminished or neutralized, and the suspension is destabilized.[42] At higher pH values, it does not show an increase in removal efficiency until pH 10. However, it is still higher than the values at pH 7-7.5. It can be concluded that the optimum removal efficiency is achieved at a dose of 20-35 g/mL with an optimum working pH between 3.5-6.

The interaction effects of mixing speed and pH on the COD removal efficiency in the treatment of APSME is shown in the 3D response surface plot and contour diagram in Figure 8, for pH 1-10 and mixing speeds of 70-150 rpm. The percentage of removal efficiency increased from 70 to 100 rpm at a working pH of 3.5-5.5, with COD removal efficiency of 60-72%. At higher mixing speeds, the removal efficiency decreases starting at 110 rpm and drops significantly at 150 rpm to a COD removal efficiency of 59.15% at an optimum pH of 5.5. This decrease is observed at a lower pH of 3.5 with a COD removal efficiency of 50.15%. This occurs because aggregated particles disperse and disturb particles settling above the optimal coagulant concentration.[42-44] With a COD removal efficiency of 71.95%, it was concluded that the optimal removal efficiency was achieved at a mixing speed of 90 rpm and a pH of 5.5.

Zeta potential profile of DSF, DSC, and DSC-G coagulants

Zeta potential is a parameter of electric charge between colloidal particles. The higher the zeta potential value, the smaller the flocculation. The floc stability depends on the zeta potential, which shows the degree of repulsion between particles of the same charge that are close to each other. A high zeta potential value will provide solution stability to resist aggregation. On the other hand, when the zeta potential is low, the attraction between the particles in the dispersion exceeds the repulsion, and flocculation occurs.[45] The zeta potential value can indicate an estimate of the coagulants' ability to form flocs when applied to APSME. The higher the zeta potential value, the smaller the flocs. Figure 9 shows the data from the zeta potential measurement. Figure 9 shows that the values of zeta potential of the flocs approached zero and had a strong charge under acid conditions, as the optimum working pH was at 5.5.

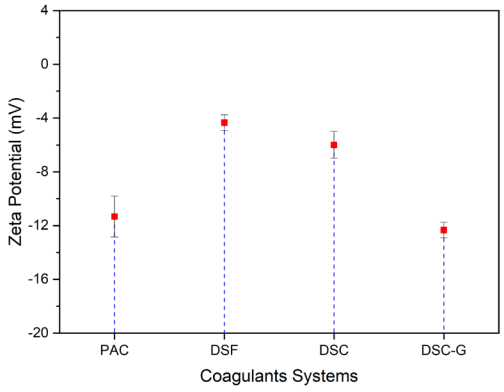

Figure 9: Effluent zeta potential in four coagulation systems at pH 5.5 and mixing speed of 90 rpm: PAC (poly aluminum chloride), DSF (durian skin flour), DSC (durian skin cellulose), and DSC-G (durian skin cellulose crosslinked with glutaraldehyde) in the treatment of APSME

The addition of coagulant reduced contaminants in APSME, which showed floc stability, as indicated by the zeta potential value. PAC and DSC-G have almost identical floc stability, with zeta potential values of -11.33 and -12.33 mV, respectively. Meanwhile, DSF and DSC have higher zeta potential values of -4.33 and -6, respectively. It is known that PAC and DSC-G coagulants tend to aggregate in dilute solutions due to the hydrogen bonds or van der Waals forces.[46,47] In addition, DSC-G has a hydroxyl group in its cellulose structure and a carbonyl group, due to the crosslinking reaction with glutaraldehyde, which could easily bind to contaminants in APSME, leading to the formation of floc aggregates.

Surface morphology of coagulants

Figure 10 depicts the surface morphology of DSC-G prior to its use as a coagulant for the treatment of APSME. DSC-G has an irregular shape and a rough surface. During the coagulation-flocculation process, a larger surface area could help provide more adsorption sites due to the rough and porous surface.[40] Intriguingly, after the coagulation-flocculation treatment, the morphology of the flocs has changed, revealing that they are neatly arranged in layers, confirming that DSC-G is well-formed and dense.[48] This change occurs because the colloidal particles in the coagulant can bind the particles in APSME.

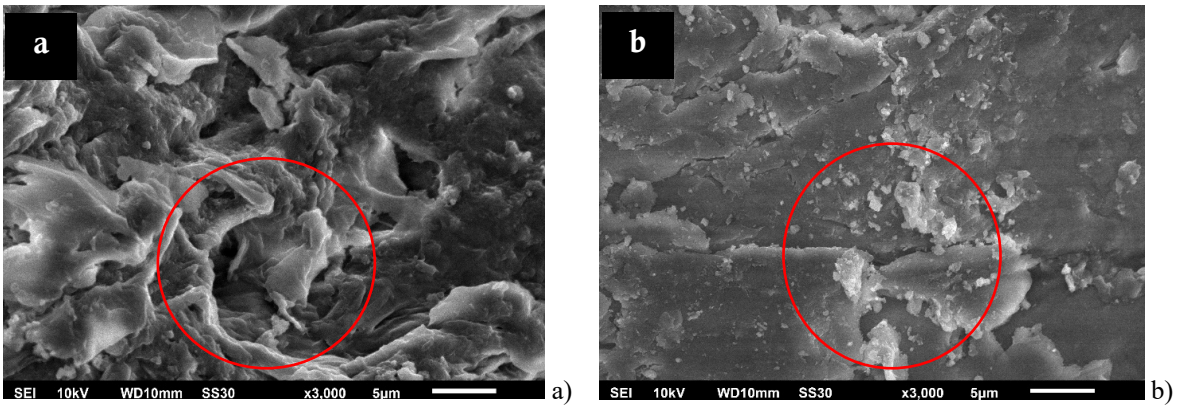

a) b)

Figure 10: SEM images at 3000x magnification of DSC-G coagulant before (a) and after (b) coagulation-flocculation treatment of APSME

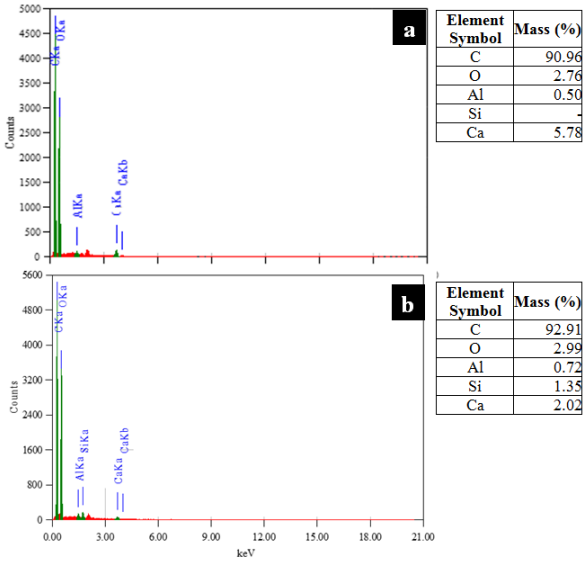

Element Symbol	Mass (%)
C	90.96
O	2.76
Al	0.50
Si	-
Ca	5.78

Element Symbol	Mass (%)
C	92.91
O	2.99
Al	0.72
Si	1.35
Ca	2.02

Figure 11: EDX spectra of DSC-G before (a) and after (b) coagulation-flocculation treatment of APSME

Energy-dispersive X-ray spectra (EDX) of DSC-G before and after the treatment process to remove contaminants from APSME areshown in Figure 11. The composition of the coagulant before and after the coagulation-flocculation treatment of APSME is shown in Table 3. As can be noted, the main component in DSC-G is carbon, derived from the cellulose structure, which is also evidenced in the FTIR spectra in Figure 1. However, it turns out that DSC-G also contains aluminum elements, similarly to PAC. In the DSC-G flocs, there was an increase in carbon and aluminum, and a decrease in calcium. This composition change indicates that DSC-G can effectively absorb contaminants from APSME. In addition, a new element, Si, is found in the DSC-G flocs, which is also thought to come from APSME.

Table 3
Elemental composition of DSC-G before and after coagulation-flocculation treatment of APSME

Compound	DSC-G (wt%)	DSC-G floc (wt%)
Carbon (C)	90.96	92.91
Oxygen (O)	2.76	2.99
Aluminum (Al)	0.50	0.72
Calcium (Ca)	5.78	2.02
Silica (Si)	-	1.35

On the basis of the surface morphology observation of DSC-G and DSC-G flocs, APSME may be adsorbed onto the active sites of the porous surface of DSC-G. The efficiency of the coagulant in the adsorption process is due to its affinity for coupling with hydroxyl groups on cellulose and carbonyl groups on glutaraldehyde.[49] As previously reported, by using GRAS (generally thought to be safe) materials, instead of traditional inorganic coagulants like alum and PAC, it is possible to treat polluted wastewater without harming ecosystems.[50]

Coagulation mechanism of durian skin cellulose crosslinked with glutaraldehyde

The modification of cellulose through a crosslinking reaction with glutaraldehyde can result in the production of cellulose, which is more effective in clumping organic waste. This process creates a denser and sturdier network within the cellulose structure, as depicted in Figure 10, which illustrates the presence of numerous large cavities. After the modification with glutaraldehyde, as shown in Figure 12, the DSC-G coagulant exhibits a higher water contact angle. This is attributed to the partial crosslinking of the hydrophilic hydroxyl groups by the aldehyde groups of glutaraldehyde. As a result, the DSC-G coagulant demonstrates superior clumping ability, compared to ordinary cellulose, which may be useful when handling organic waste.

Based on the illustration in Figure 13, when a large amount of coagulant is mixed into wastewater, it precipitates in the form of hydroxide. This process, known as sweep coagulation/flocculation, causes the colloidal particles dissolved in water to be trapped by the coagulant precipitate. This mechanism effectively removes particles destabilized by neutralization of charge, as it shows a better aggregation rate with increased solid concentration. This process is beneficial for removing harmful compounds[51,52] and is employed in this work in treating APSME with DSC-G coagulant.

APSME, like other colloidal systems, is stable when individual particles are dispersed. This stability is due to forces keeping the particles apart, preventing aggregation.[53] In most aqueous systems, the primary mechanism for colloid stability is charge stabilization, which prevents aggregation due to electrostatic repulsion between similarly charged particles.[54]

The DSC-G coagulant, a natural polymer, contains charged and functional groups, particularly hydroxyl (–OH) functional groups, as depicted in Figure 12, which drive the aggregation and coagulation process similar to polyelectrolytes. In the coagulation process, coagulants bridge, neutralize the charge, and sweep coagulate, compressing the electrical double layer of charged colloidal particles.[55,56] When the DSC-G coagulant is added to the wastewater, charged particles can approach the

van der Waals contact distance, leading to aggregation.[54,57]

The pH of the water system significantly influences the aggregation process. Alterations in pH can impact the nature of APSME and the efficiency of the coagulation processes. Increasing the pH enhances the aggregation process due to the presence of hydroxyl functional groups in the DSC-G coagulant.[58,59] These colloids can adsorb other soluble species, causing charge neutralization and destabilization in suspended colloidal systems. Under appropriate conditions, van der Waals and electrostatic forces force flocculation into larger flocs or aggregates.[60,61]

The structure of the DSC-G coagulant, a polymer, influences the formation of floc aggregates. It can adsorb to particles in suspension and form bridges between them, which are not easily reversed.[62,63] Additionally, the DSC-G coagulants possess hydrogen atoms covalently bound to electronegative atoms or groups (hydrogen bond donors), such as hydroxyl functional groups, which can make hydrogen bonds with other electronegative atoms in APSME or mineral hydroxide surfaces.[62-64]

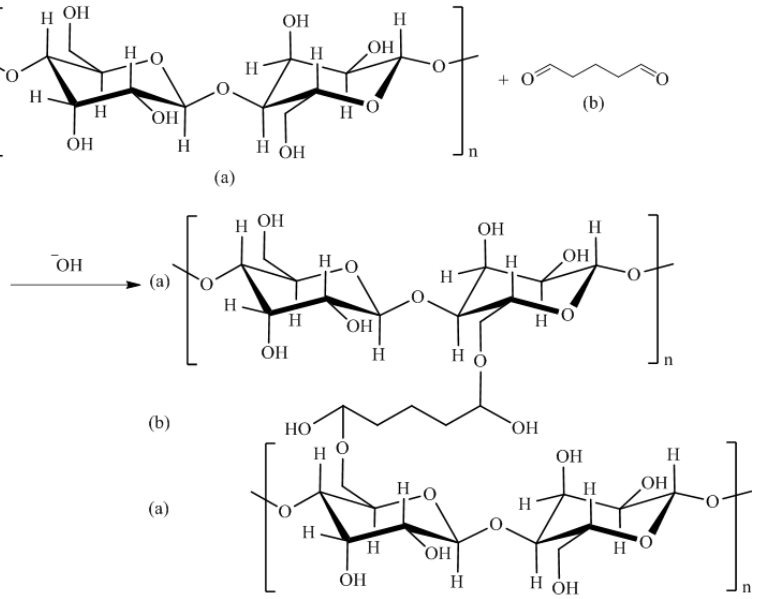

Figure 12: Illustration of crosslinking reaction between (a) durian skin cellulose and (b) glutaraldehyde

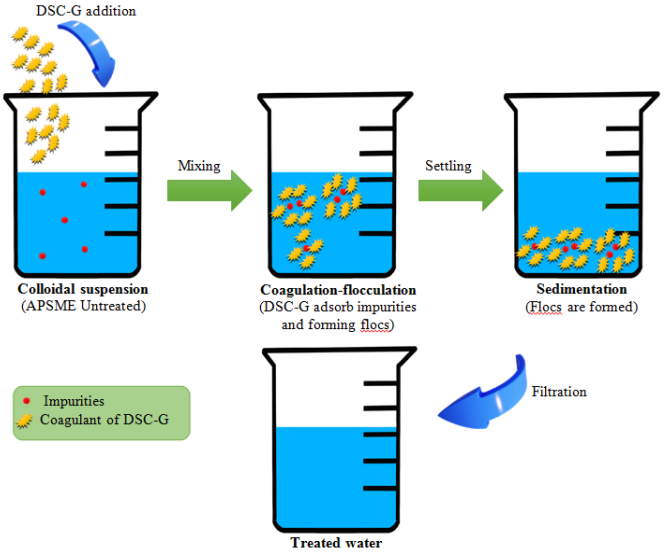

Figure 13: Illustration of coagulation-flocculation treatment of APSME using DSC-G coagulant

As a long-chain polymer, the DSC-G coagulant interacts with APSME through polymer bridging. The concentration of the DSC-G coagulant affects this interaction: a too high concentration may cover particle surfaces in APSME, reducing bridging contact, while a too low concentration may result in few bridging contacts.[65] Therefore, there is an optimum dosing range for DSC-G coagulant in a given system.[64,65] This study found that the optimal DSC-G concentration was 2500 mg/L, at an optimal working pH of 5.5 and a mixing speed of 90 rpm. This mechanism works in the treatment of APSME by the DSC-G coagulant.

CONCLUSION

Reducing the polluting effects of APSME generated by APS industrial centers in Klaten, Central Java, Indonesia, with a natural coagulant DSC-G, synthesized from durian skin cellulose through a crosslinking reaction with glutaraldehyde, has been evaluated. Several coagulants were compared for determining their efficiciency: DSC-G, DSF, DSC and synthetic coagulant PAC. The study determined that the process efficiency in terms of the percentage removal for COD, BOD_5, TDS, and TSS, and the maximum values were obtained for DSC-G of 71.38%, 78.23%, 94.79%, and 96.12%, with a sludge volume percentage of 24%. The optimal DSC-G concentration was determined to be 2500 mg/L, with an optimal working pH of 5.5 and a mixing speed of 90 rpm. The floc stability of DSC-G is -12.33 mV. This study indicates that DSC-G may be utilized as a coagulant in the treatment of APSME.

ACKNOWLEDGMENT: This research was funded by The Institute for Research and Community Service at Universitas Negeri Semarang. The institute sponsored the research activities through the DPA LPPM Universitas Negeri Semarang funds, under the basic research scheme with contract number 26.12.4/UN37/PPK.10/2023.

REFERENCES

[1] D. R. Adawiyah, S. Akuzawa, T. Sasaki and K. Kohyama, *J. Food Sci. Technol.*, **54**, 3404 (2017), https://doi.org/10.1007/s13197-017-2787-1

[2] M. L. Sanyang, S. M. Sapuan, M. Jawaid, M. R. Ishak and J. Sahari, *Renew. Sustain. Energ. Rev.*, **54**, 533 (2016), https://doi.org/10.1016/j.rser.2015.10.037

[3] M. L. Sanyang, S. M. Sapuan, M. Jawaid, M. R. Ishak and J. Sahari, *J. Food Sci. Technol.*, **53**, 326 (2015), https://doi.org/10.1007/s13197-015-2009-7

[4] J. Sahari, S. M. Sapuan, E. S. Zainudin and M. A. Maleque, *Carbohyd. Polym.*, **92**, 1711 (2013), https://doi.org/10.1016/j.carbpol.2012.11.031

[5] M. R. Ishak, S. M. Sapuan, Z. Leman, M. Z. A. Rahman, U. M. K. Anwar *et al*., *Carbohyd. Polym.*, **91**, 699 (2013), https://doi:10.1016/j.carbpol.2012.07.073

[6] Directorate General of Plantations, Area and plantation size throughout Indonesia according to province and business status, Department of Agriculture, Jakarta, 2021. https://ditjenbun.pertanian.go.id/template/uploads/2022/08/STATISTIK-UNGGULAN-2020-2022.pdf

[7] D. R. Adawiyah, T. Sasaki and K. Kohyama, *Carbohyd. Polym.*, **92**, 2306 (2013), https://doi.org/10.1016/j.carbpol.2012.12.014

[8] M. Firdayati and M. Handajani, *Infrastruktur dan Lingkungan Binaan*, **1**, 22 (2005), https://api.semanticscholar.org/CorpusID:192148641

[9] A. K. Verma, R. R. Dash and P. Bhunia, *J. Environ. Manage.*, **93**, 154 (2012), https://doi.org/10.1016/j.jenvman.2011.09.012

[10] A. H. Jagaba, A. A. Latiff, I. Umaru, S. Abubakar and I. M. Lawal, *IOSR J. Mech. Civ. Eng.*, **13**, 67 (2016), https://doi.org/10.9790/1684-1306076775

[11] D. S. N. Hendrawati, *Valensi*, **3**, 23 (2013), https://doi.org/10.15408/jkv.v3i1.326

[12] D. Alighiri, S. Wardani and Harjito, *Proceeding Seminar Nasional Kimia dan Pendidikan Kimia SNKPK*, **1**, 28 (2015)

[13] Masturi, D. Alighiri, P. Dwijananti, R. W. Widodo, S. P. Budiyanto *et al*., *JBAT*, **9**, 36 (2020), https://doi.org/10.15294/jbat.v9i1.23574

[14] Masturi, D. Alighiri, S. S. Edie, A. Drastisianti, U. Khasanah *et al*., *J. Phys.*, **1567**, 042084 (2020), https://doi:10.1088/1742-6596/1567/4/042084

[15] S. R. Masrol, M. H. I. Ibrahim and S. Adnan, *Proc. Manuf.*, **2**, 171 (2015), https://doi:10.1016/j.promfg.2015.07.030

[16] H. B. Aditiya, T. M. I. Mahlia, W. T. Chong, H. Nur and A. H. Sebayang, *Renew. Sustain. Energ. Rev.*, **66**, 631 (2016), https://doi:10.1016/j.rser.2016.07.015

[17] Y. L. Tan, A. Z. Abdullah and B. H. Hameed, *Bioresour. Technol.*, **243**, 85 (2017), https://doi.org/10.1016/j.biortech.2017.06.015

[18] H. Li, Z. Wang, X. Liu, F. Cui, C. Chen *et al*., *Chem. Phys. Lett.*, **755**, 137805 (2020), https://doi:10.1016/j.cplett.2020.137805

[19] A. H. Jagaba, S. R. M. Kutty, G. Hayder, A. A. A. Latiff, N. A. A. Aziz *et al*., *Ain Shams Eng. J.*, **11**, 951 (2020), https://doi:10.1016/j.asej.2020.01.018

[20] Nur'ain, Nurhaeni and A. Ridhay, *Kovalen*, **3**, 112 (2017), https://doi.org/10.22487/j24775398.2017.v3.i2.8717
[21] S. Hong, J. Lee and S. Son, *Packag. Technol. Sci.*, **18**, 1 (2005), https://doi.org/10.1002/pts.667
[22] F. M. Plieva, M. Karlsson, M. R. Aguilar, D. Gonez, S. Mikhalovsky *et al*., *J. Appl. Polym. Sci*., **100**, 1057 (2006), https://doi.org/10.1002/app.23200
[23] A. I. Abdillah, Darjito and M. M. Khunur, *Kimia Student*, **1**, 826 (2015), http://kimia.studentjournal.ub.ac.id/index.php/jikub/article/view/619
[24] J. M. Thompson, "Infrared Spectroscopy", Pan Stanford Publishing, Singapore, 2018, https://doi.org/10.1201/9781351206037
[25] APHA, Standard Methods for the Examination of Water and Wastewater, 21st ed., American Public Health Association, Washington DC, 2005
[26] AOAC, Official Methods of Analysis, 14th ed., Association of Official Analytical Chemist, USA, 1993
[27] Indonesian National Standards, Water and Wastewater-Part 2: How to test chemical oxygen demand (COD) with closed reflux spectrophotometrically, SNI 6989.2:2019, National Standardization Agency of Indonesia, Jakarta, 2019, http://sispk.bsn.go.id/sni/DetailSNI/12250
[28] Indonesian National Standards, Water and Wastewater-Part 27: How to test total dissolved solids (TDS) gravimetrically, SNI 6989.27:2019, National Standardization Agency of Indonesia, Jakarta, 2019, http://sispk.bsn.go.id/SNI/DetailSNI/12249
[29] Indonesian National Standards, Water and Wastewater-Part 72: How to test biochemical oxygen demand (BOD), SNI 6968.72:2009, National Standardization Agency of Indonesia, Jakarta, 2009, https://pesta.bsn.go.id/produk/detail/8217-sni6989722009
[30] Indonesian National Standards, Water and Wastewater-Part 23: How to test temperature with a thermometer, SNI 06-6989.23-2005, National Standardization Agency of Indonesia, Jakarta, 2005, https://pesta.bsn.go.id/produk/detail/6996-sni06-698923-2005
[31] Indonesian National Standards, Water and Wastewater-Part 3: How to test total suspended solids (TSS) gravimetrically, SNI 06-6989.3:2004, National Standardization Agency of Indonesia, Jakarta, 2004, http://sispk.bsn.go.id/sni/DetailSNI/12245
[32] Indonesian National Standards, Water and Wastewater-Part 3: How to test the degree of acidity (pH) using a pH meter, SNI 06-6989.11-2004, National Standardization Agency of Indonesia, Jakarta, 2004, http://sispk.bsn.go.id/SNI/DetailSNI/6816
[33] M. S. Yusoff, H. A. Aziz, M. F. M. A. Zamri, F. Suja, A. Z. Abdullah *et al*., *Waste Manage*., **74**, 362 (2018), https://doi.org/10.1016/j.wasman.2018.01.016
[34] M. S. Reid, M. Villalobos and E. D. Cranston, *Langmuir*, **33**, 1583 (2017), https://doi.org/10.1021/acs.langmuir.6b03765
[35] P. Lestari, N. H. Titi, H. I. L. Siti and W. M. Djagal, "Development Technology Creation Biopolymers High Economic Value of Waste Corn Plant (Zea mays) For Food Industry: CMC (Carboxy Methyl Cellulose)", Universitas Gajah Mada, Yogyakarta, 2014
[36] B. Liu, C. Du, J. J. Chen, J. Y. Zhai, Y. Wang *et al*., *Chem. Phys. Lett*., **771**, 138535 (2021), https://doi:10.1016/j.cplett.2021.138535
[37] A. Leena, C. Meiaraj and D. N. Balasundaram, *IOSR J. Mech. Civil. Eng*. (*IOSR-JMCE*), 2278 (2016), https://doi.org/10.9790/1684-130508107114
[38] M. Abdulsalam, H. C. Man, A. I. Idris, K. F. Yunos and Z. Z. Abidin, *Water*, **10**, 1165 (2018), https://doi:10.3390/w10091165
[39] M. M. Sarafraz and F. Hormozi, *Ain Shams Eng. J*., **5**, 553 (2014), https://doi.org/10.1016/j.asej.2013.11.006
[40] H. Patel and R. T. Vashi, *Global NEST. J*., **15**, 522 (2013), https://journal.gnest.org/sites/default/files/Submissions/1002/1002_published.pdf
[41] W. Subramonian and T. Y. Wu, *Water Air Soil Pollut*., **225**, 1 (2014), https://doi.org/10.1007/s11270-014-1922-0
[42] B. Tawakkoly, A. Alizadehdakhel and F. Dorosti, *Ind. Crop. Prod*., **137**, 323 (2019), https://doi:10.1016/j.indcrop.2019.05.038
[43] A. Mishra and M. Bajpai, *J. Hazard. Mater*., **118**, 213 (2005), https://doi.org/10.1016/j.jhazmat.2004.11.003
[44] C. Y. Teh, T. Y. Wu and J. C. Juan, *Ecol. Eng*., **71**, 509 (2014), https://doi.org/10.1016/j.ecoleng.2014.07.005
[45] R. J. Hunter, "Zeta Potential in Colloid Science: Principles and Applications", Academic Press, Australia, 2013
[46] C. Shen, Y. Pan, D. Wu, Y. Liu, C. Ma *et al*., *Chem. Eng. J*., **374**, 904 (2019), https://doi.org/10.1016/j.cej.2019.05.203
[47] Q. Feng, B. Gao, Q. Yue and K. Guo, *Chemosphere*, **262**, 128416 (2021), https://doi:10.1016/j.chemosphere.2020.128416
[48] S. Mukherjee, S. Mukhopadhyay, M. Z. B. Zafri, X. Zhan, M. A. Hashim *et al*., *Ind. Crop. Prod*., **111**, 261 (2018), https://doi.org/10.1016/j.indcrop.2017.10.022
[49] G. Sharma, S. Sharma, A. Kumar, A. H. Al-Muhtaseb, M. Naushad *et al*., *Carbohyd. Polym*., **199**, 534 (2018), https://doi.org/10.1016/j.carbpol.2018.07.053
[50] M. Srivastava and V. Kapoor, *Chem. Biodivers*., **2**, 295 (2005), https://doi.org/10.1002/cbdv.200590013

[51] M. Sciban, M. Klasnja and J. Stojimirovic, *Acta Period. Technol.*, **36**, 81 (2005), http://dx.doi.org/10.2298/APT0536081S
[52] A. Nath, A. Mishra and P. P. Pande, *Mater. Today: Proc.*, **46**, 6113 (2021), https://doi.org/10.1016/j.matpr.2020.03.551
[53] Y. Lan, A. Caciagli, G. Guidetti, Z. Yu, J. Liu *et al.*, *Nat. Commun.*, **9**, 3614 (2018), https://doi.org/10.1038/s41467-018-05560-3
[54] H. Xu, H. Lin, H. Jiang and L. Guo, *Water Res.*, **144**, 543 (2018), https://doi.org/10.1016/j.watres.2018.07.075
[55] M. Adinofi, M. M. Corsaro, R. Lanzetta and M. Parrilli, *Carbohyd. Res.*, **263**, 103 (1994), https://10.1016/0008-6215(94)00149-9
[56] P. M. Badot, G. Crini, F. Renault and B. Sancey, *Eur. Polym. J.*, **45**, 1337 (2009), https://doi.org/10.1016/j.eurpolymj.2008.12.027
[57] B. Bolto and J. Gregory, *Water. Res.*, **41**, 2301 (2007), https://doi.org/10.1016/j.watres.2007.03.012
[58] J. Duan and J. Gregory, *Adv. Colloid Interface Sci.*, **100–102**, 475 (2003), https://doi.org/10.1016/S0001-8686(02)00067-2
[59] J. Q. Jiang, *Curr. Opin. Chem. Eng.*, **8**, 36 (2015), https://doi.org/10.1016/j.coche.2015.01.008
[60] P. A. Reynolds and C. A. Reid, *Langmuir*, **7**, 89 (1991), https://doi.org/10.1021/la00049a018
[61] L. Chekli, C. Eripret, S. H. Park, S. A. A. Tabatabai, O. Vronska *et al.*, *Sep. Purif. Technol.*, **175**, 99 (2017), https://doi.org/10.1016/J.SEPPUR.2016.11.019
[62] S. Tang, L. Gao, T. Zhao and A. Tian, *J. Water Process Eng.*, **57**, 104630 (2024), https://doi.org/10.1016/j.jwpe.2023.104630
[63] B. A. Bolto, *Prog. Polym. Sci.*, **20**, 987 (1995), https://doi.org/10.1016/0079-6700(95)00010-D
[64] J. F. Lee, P. M. Liao, D. H. Tseng and P. T. Wen, *Chemosphere*, **37**, 1045 (1998), https://doi.org/10.1016/S0045-6535(98)00102-7
[65] L. Lundström-Hämälää, E. Johansson and L. Wagberg, *Starch/Staerke*, **62**, 102 (2010), https://doi.org/10.1002/star.200900176